JASA Express Letters

MARCH 01 2023

Open ocean ambient noise data in the frequency band of 100 Hz–50 kHz from the Pacific Ocean

Jie Yang; Jeffery A. Nystuen; Stephen C. Riser; Eric I. Thorsos

JASA Express Lett. 3, 036001 (2023)
https://doi.org/10.1121/10.0017349

JASA EXPRESS LETTERS ARTICLE asa.scitation.org/journal/jel

Open ocean ambient noise data in the frequency band of 100 Hz–50 kHz from the Pacific Ocean

Jie Yang,[1] Jeffery A. Nystuen,[1,a)] Stephen C. Riser,[2] and Eric I. Thorsos[1]
[1]Applied Physics Laboratory, University of Washington, Seattle, Washington 98105, USA
[2]School of Oceanography, University of Washington, Seattle, Washington 98105, USA
jieyang@uw.edu, riser@ocean.washington.edu, eit@apl.washington.edu

Abstract: Bubbles from wind generated breaking surface waves are the dominant ambient noise source [Dean and Stokes, Nature **418**, 839–844 (2002)]. With ambient noise data collected in the open ocean between 100 Hz and 50 kHz from 1999 to 2022, the ambient noise level is observed to sharply decrease as wind speed increases beyond 15 m/s for frequencies higher than 4 kHz. Data-model comparisons show a mismatch, as existing models including the Wenz curves [Wenz, J. Acoust. Soc. Am. **34**, 1936–1956 (1962)] are monotonic in nature. The decrease at high wind speeds and frequencies is likely due to attenuation when ambient sound propagates through the deeper and denser bubble layer for high sea conditions [Farmer and Lemon, J. Phys. Oceanogr. **14**, 1761–1777 (1984)].

[Editor: David R Dall'Osto] https://doi.org/10.1121/10.0017349

Received: 2 November 2022 **Accepted:** 2 February 2023 **Published Online:** 1 March 2023

1. Introduction

Ocean ambient noise, spanning from a few hertz to tens of kilohertz, is often the limiting factor for sonar performance in target detection, location, and identification. The ambient noise field changes constantly over time and space, posing challenges to the fidelity of operational algorithms, and therefore demands understanding of the underlying physics of the noise field for prediction purposes.

The underwater ambient sound field consists of sound produced by biological (e.g., marine mammals, snapping shrimp), anthropogenic (e.g., shipping), and geophysical (e.g., rainfall, near surface bubbles from breaking waves) processes. (For simplicity, the ambient sound field produced by wind forcing that leads to breaking waves and near surface bubble clouds will be referred to as a result of wind forcing or simply as due to the wind.) These noise sources work in different frequency bands, with some overlap.[1–3] For frequencies relevant to naval operations, i.e., O(100 Hz)–20 kHz, ambient noise mainly comes from two sources: wind forcing and rainfall events, especially the former.[4] Wind forcing leads to ambient noise from resonant bubble radiation for frequencies above several kilohertz, and collective oscillations of bubble clouds may lead to ambient noise at much lower frequencies.[5] Since the time rain falls over the ocean is in general in the range of 10% to 20%,[6] this paper will focus on ambient noise data due to wind forcing, as done with the Wenz curves, with data obtained during rain excluded.

The ambient noise data presented in this work were recorded using the passive aquatic listener[7] (PAL) on deep ocean moorings without possible complications seen in littoral oceans. Data come from six different locations of the Pacific Ocean over two decades and have companion surface meteorological data including wind speed and rain rate.[8,9] With the 2-decade ambient noise data from 1999 to 2022, the goal here is to summarize data as a function of wind speed and compare with predictions from ambient noise models.

This paper is organized as follows. Section 2 describes the ambient noise measurement technique used in this work and presents ambient noise data. Representative ambient noise models are discussed and compared with ambient noise data in Sec. 3, followed by a Summary.

2. Ambient noise data

Ambient noise data presented in this work were recorded using the PAL. PAL is a self-contained system with a hydrophone, processing unit, and battery pack in a pressure case that can be deployed on ocean moorings. Data came from six deep ocean moorings in the Pacific Ocean, spanning 1999–2022.

2.1 Technique and measurement platform: PAL

PAL, formerly called an acoustic rain gauge,[7] consists of a broadband, low noise hydrophone, a signal processing board, a low-power microprocessor with a 100 kHz A/D digitizer, a 32 Gbyte memory card, and a battery pack. PAL records a

[a)]Deceased.

4.5-s ambient noise time series and converts that to a frequency spectrum over the frequency range of 100 Hz–50 kHz. Ambient noise levels at 64 selected frequencies (specified in Ref. 10) ranging from 100 Hz to 50 kHz are saved for later analysis.

PAL has been designed and used for different applications, including marine mammal monitoring and wind speed and rain rate estimation for studies of processes such as the global water cycle.[9] PAL does adaptive data recording depending on environmental conditions.[11] For example, PAL records data every 2 min when a rain event is detected or every 8 min when the predominant noise source is due to wind forcing. The longest data sampling interval is 10 min in this work.

2.2 Ambient noise data on deep ocean moorings

The multi-year data presented here are from three major efforts: NOAA Tropical Atmosphere Ocean[12] (TAO), NOAA Ocean Climate Stations at PAPA[13] (OCS PAPA), and NASA Salinity Processes in the Upper-ocean Regional Study phase 2 field campaign[9] (SPURS-2). Table 1 summarizes location, residence time, site water depth, and PAL deployment depth for each data set. In particular, data from 1999 to 2003 are from the NOAA's TAO array in the tropical Pacific Ocean (8°N, 10°N, and 12°N, 95°W, see Table 1); the 2007–2022 data at 50°N 145°W are supported by NOAA's OCS project; and the 2016–17 data at 10°N and 9°N, 125°W are part of the NASA's SPURS-2 field effort.

An example of PAL recorded ambient noise data is shown in Fig. 1, using data from 10°N 125°W, at 1000 m depth. This spectrogram covers a week of ambient noise data in the frequency band of 100 Hz–50 kHz. Surface measurements of wind speed (in blue, m/s) and rain rate (in red, rain rate in mm/h + 20 for display purposes) are provided by NASA and overlaid with acoustics to show their correlation. As mentioned, rain and wind forcing are the dominant geophysical ambient noise sources.[2,10,11] As shown in Fig. 1, there are episodes of high noise that are dominated by rain, which are precisely confirmed by surface rain rate measurements (red curve). Rain induced ambient noise can overwhelm that generated by surface breaking waves, as in Fig. 1. For the following analysis, all data taken during rainy periods are removed using surface rain rate measurements. In addition to rain events, it can be seen from Fig. 1 that wind speed and background ambient noise intensity level are very well correlated, i.e., higher wind speed correlates with higher background intensity.

Over the course of two decades, a total of about 1.35×10^6 ambient noise samples, i.e., sound pressure level (SPL) from 100 Hz to 50 kHz, were obtained from locations listed in Table 1. With rain events excluded, the ambient noise data are sorted according to wind speed. Wind speed ranges of 1–3, 6–8, 11–13, 15–17, 18–20, and 21–23 m/s are chosen to represent surface conditions from calm to the start of wave breaking and to very rough seas. Maximum wind speed is about 23 m/s for the collective data set. The spectra recorded under each wind speed range are intensity averaged and the results are shown in Fig. 2(a). Note, water absorption has been taken out from PAL ambient noise data presented in this work so that ambient noise data taken at different depths can be compared. This change makes at most 1 dB difference at 20 kHz and much less at lower frequencies.

The averaged spectra from PAL are shown with solid curves for the six wind speed ranges. For frequency $\lesssim$4 kHz, the sound pressure level (SPL) increases with wind speed and a considerable increase in SPL can be seen at all frequencies between the calm sea (1–3 m/s) and 6–8 m/s, when surface waves start to break. This elevation in SPL starts to

Table 1. All historical PAL data on deep ocean moorings.

GPS location	Residence time	Water depth (m)	Hydrophone depth (m)
8°N 95°W (TAO)	10/30/1999–3/19/2000	3690	38
	4/23/2000–11/9/2000		38
	11/22/2001–10/14/2002		38
10°N 95°W (TAO)	12/1/1999–4/1/2000	3875	38
	5/7/2000–10/13/2000		38
	11/12/2000–10/12/2002		38
	10/18/2002–10/26/2003		38
12°N 95°W (TAO)	4/21/2000–12/31/2000	4130	38
	4/25/2001–3/31/2002		38
50°N 145°W (Ocean Station PAPA)	6/6/2007–6/12/2009	4220	500
	6/16/2009–1/10/2010		500
	6/29/2010–8/5/2013		500
	12/14/2019–5/21/2022		200
10°N 125°W (SPURS-2)	8/20/2016–6/22/2017	4600	500
	8/20/2016–6/30/2017		1000
9°N 125°W (SPURS-2)	8/20/2016–6/22/2017	4686	650

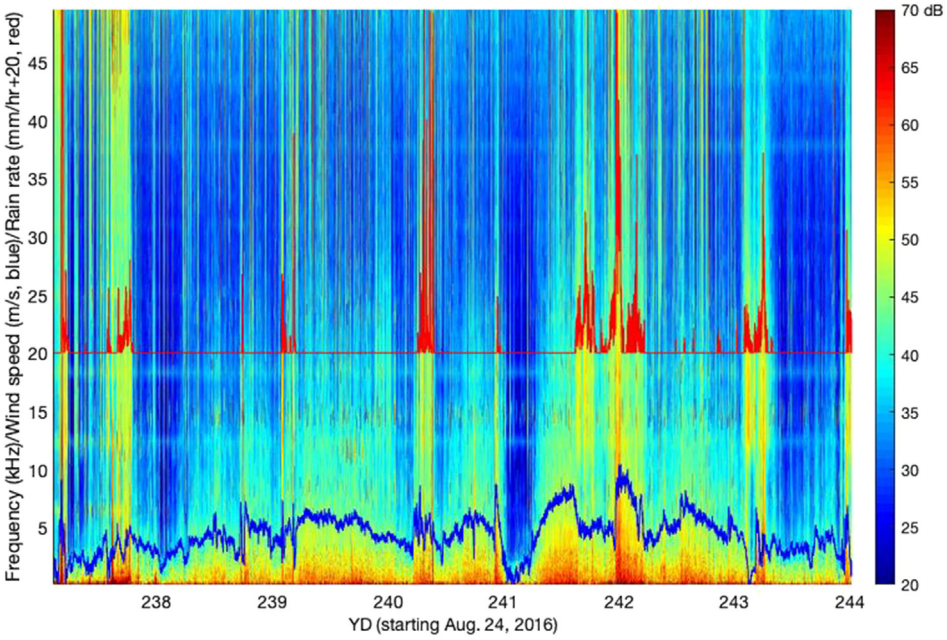

Fig. 1. Sample ambient noise data from 10°N, 125°W in Table 1 with surface wind speed (blue, in m/s) and rain rate (red, in mm/h + 20 for display purposes). YD: yearday.

break down between 11–13 and 15–17 m/s cases, where a sharp drop-off for frequencies higher than 4 kHz is observed and the SPL can fall below that of much lower wind speed. The most extreme is the 21–23 m/s case with a sharp falloff starting from 4 kHz, with the SPL above 20 kHz approaching a similar level as the relatively calm sea case. (Note, the small spectral peak around 40 kHz is from the instrument.)

With the mean levels established, it is important to look at variations in this collective data set. Figure 2(b) shows the mean spectral levels for wind speed ranges of 6–8, 15–17, and 21–23 m/s with corresponding standard deviations. It is only for the purpose of display that three wind speed ranges are shown instead of six as in Fig. 2(a). From low to high wind speed, the mean and standard deviation results are based on 300 000, 10 000, and 1600 data samples, respectively. The standard deviations have been obtained using levels expressed in dB. Interestingly, all three cases yield similar standard deviations of about 2–3 dB.

The histogram in Fig. 2(c) shows about 80% of data are within 3 dB of the mean. The histogram uses data for 6–8 m/s wind speed conditions at 5 kHz, and for these conditions the ambient noise level has been demonstrated to correlate well with wind speed.[14] Similar histograms have been obtained for wind-induced ambient noise level at 5 kHz for different wind speed ranges. It is found that as wind speed increases, the maximum spread in the data, i.e., difference between maximum and minimum ambient noise levels, decreases. Specifically, for the 6–8 m/s case, the maximum spread in the data at 5 kHz is 57 dB [Fig. 2(c)], while the corresponding spread for 11–13, 15–17, 18–20, and 21–23 m/s are 27, 20, 16, and 14 dB, respectively. The well-defined Gaussian shape histogram seen in Fig. 2(c) starts to break down when wind speed exceeds 17 m/s, with the resulting shape being more irregular.

3. Ambient noise data-model comparison

3.1 Representative ambient noise models

The ambient noise models of interest to this work are the ones capable of predicting noise levels due to changing surface conditions as the wind speed varies. Quite a few models, including the well-known Cron-Sherman,[15] Chapman,[16] Buckingham,[17] Plaisant,[18] and Kuperman-Ingenito[19] (K-I) predict noise level relative to unit source level (SL). To compare with *in situ* data, such models need to be combined with a model for the source level. Examples of models for which source levels have been incorporated and thus have the capability of predicting absolute levels are RANDI III,[20] CANARY,[21] and Wilson.[22] RANDI III uses the normal mode model from K-I and has specified wind generated SLs from Wilson[22] for 10–60 kn of wind speed in the frequency range of 10–1000 Hz. CANARY, based on ray theory, is built upon RANDI III's existing source levels but extended to a wider frequency range and wind speed. RANDI III and CANARY can be applied in both deep and shallow water with options of entering bottom geoacoustic properties for the latter case. The three models are inter-related and Wilson's model and an approximate model based on the source used with CANARY are chosen to compare with the PAL data. Wilson's model assumes that the ambient noise source intensity can be written as $S(f, U)\sin^2\theta$, where θ is the grazing angle with $S(f, U)$ the source density depending on frequency and wind

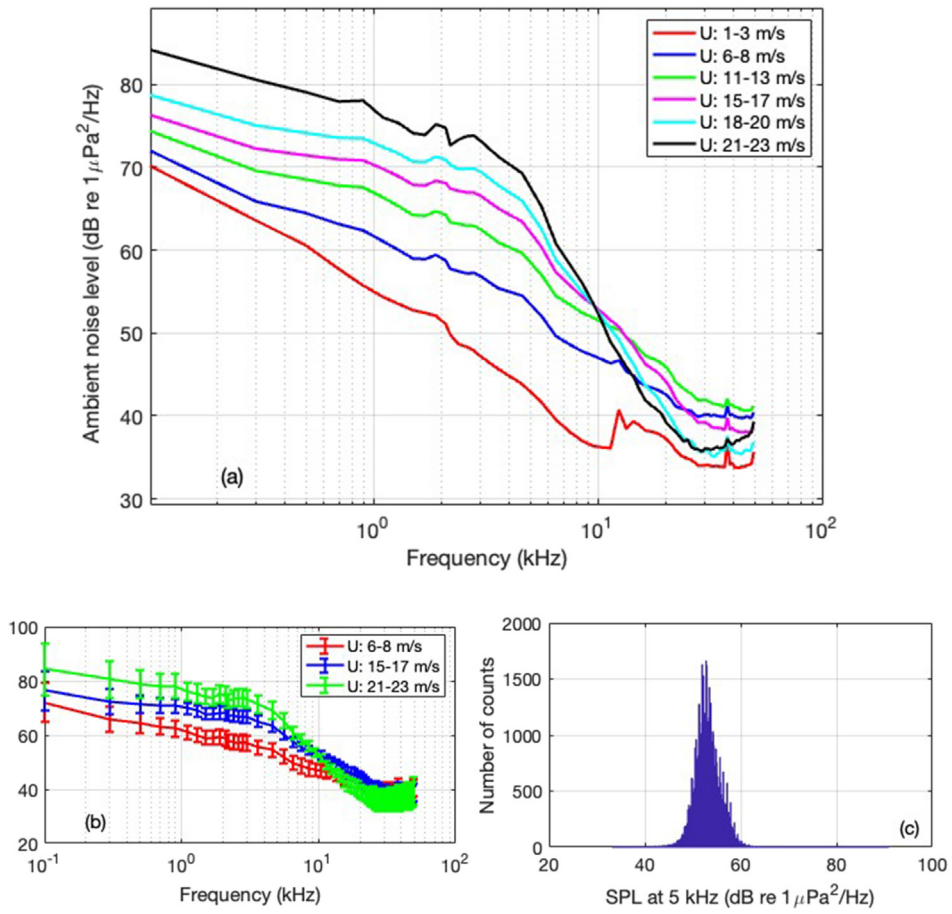

Fig. 2. (a) Solid curves: averaged ambient noise spectra recorded by a PAL in the wind speed ranges of 1–3, 6–8, 11–13, 15–17, 18–20, and 21–23 m/s using data from Table 1. (b) Mean ambient noise spectra in the wind speed ranges of 6–8, 15–17, and 21–23 m/s with respective standard deviations. The three wind speed ranges have 300 000, 10 000, and 1600 data samples, respectively. (c) Histogram of 6–8 m/s wind speed ambient noise level at 5 kHz [using data in red in (b)] with a well-defined peak centered near 53 dB. Note, water absorption has been taken out from PAL data.

speed. For the simplest scenario when only direct paths are important (no complication from ocean boundaries) in an iso-velocity environment, which is close to the measurement conditions for the collective data set presented in this work, and when water attenuation is ignored, the ambient noise intensity is obtained simply as $N(f, U) = \pi S(f, U)$. In the CANARY model, the noise source level density (in dB) is given by Eq. (21) in Ref. 21. In the approximate model employed here for $f > 1$ kHz, the same simplifying assumptions mentioned above are assumed, and the ambient noise level (in dB) is obtained by adding $10 \log \pi$ to the CANARY noise source level. While this procedure does not use the ray tracing methods of the CANARY model, the result for simplicity will be referred to as from the CANARY model, since the CANARY model would yield the results given with the assumptions being made.

3.2 Ambient noise data model comparison

In Fig. 3, the collective PAL data are compared with two models: Wilson (in circles from 100 to 1000 Hz) and CANARY (in crosses from 0.1 to 50 kHz). Wilson predicts wind generated noise level from 10 to 50 kn (5.1–25.7 m/s) with 5-kn wind speed increments, and its levels are interpolated to compare with PAL data for wind speeds of 6–8, 11–13, 15–17, 18–20, and 21–23 m/s. Both Wilson and CANARY compare well with PAL data for medium wind speeds, i.e., wind speed from 11 to 20 m/s, but are lower for the relatively calm and rough cases. For spectral slopes, both models and the PAL are similar in the band of 100–1000 Hz. For frequency higher than 4 kHz, the wind speed and frequency dependences observed in PAL data, however, cannot be described by CANARY, which predicts SPL increases with wind speed monotonically across all frequencies, just like the Wenz curves. Current monotonic models do not predict the fast drop-off of SPL for frequency higher than 4 kHz when wind speed exceeds ~15 m/s. The fast drop-off results in a "crossover" of SPL curves, i.e., the SPL for higher wind speeds is lower than that at lower wind speeds, for frequency higher than about 10 kHz.

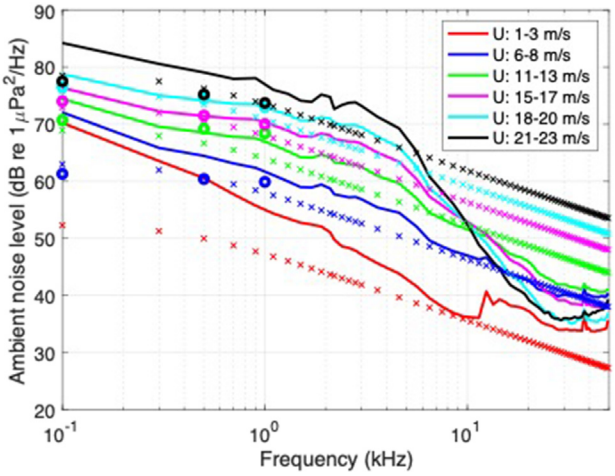

Fig. 3. Solid curves: averaged ambient noise spectra recorded by a PAL in the wind speed ranges of 1–3, 6–8, 11–13, 15–17, 18–20, and 21–23 m/s using data from Table 1. Existing models with absolute level prediction capability, Wilson[22] (in circles) and CANARY (in crosses), are compared. (Note, the peak near 15 kHz at 1–3 m/s is from drizzle and the small peak at 40 kHz is from the instrument.)

3.3 Discussion on ambient noise level versus wind speed and update of the Wenz curves

It is known that the ambient noise level correlates well with wind speed due to the resonant acoustic radiation from bubbles generated by breaking waves.[23] The bubble population size distribution defines the shape of the spectra, and the wind speed sets the amplitude by controlling the fractional area coverage of breaking waves. As wind speed increases, the total bubble concentration increases as the fractional area coverage of breaking waves increases. The increase in bubble concentration leads to a concomitant increase in the ambient noise level across all frequencies.

This correlation allows the ambient noise level at a discrete frequency to be used to infer wind speed,[14] but only for wind speed lower than ∼15 m/s. As wind speed exceeds ∼15 m/s, higher wind speeds result in a decreased ambient noise level for frequency higher than about 10 kHz as shown in Fig. 3. A decrease in ambient noise level as the wind speed increases has been reported previously using wideband data from 10 Hz to 20 kHz,[24] and measurements at single frequencies: 8, 14.5, and 25 kHz.[3]

The Wenz curves are the most popular empirical model widely used to this day and, interestingly, show only a monotonic increase in ambient noise level as the wind speed increases. A review of Ref. 2 and the data the Wenz curves are based on reveal that there is actually no inconsistency between the Wenz data and the results here or in Refs. 3 and 24.

A comparison of data from Refs. 2, 3, 24, and this work is presented in Fig. 4, with the four panels representing surface conditions of Beaufort scale 2, 3, 5, and 8. The case of comparison here is specified as in Ref. 2 [Fig. 2(b)], a deep ocean scenario. The Wenz curves are converted to units that are commonly used now,[25] resulting in a 26-dB elevation. It is found, however, that an additional 7 dB is needed to elevate the Wenz curves to compare with the other data sets across multiple Beaufort scale conditions. For comparison purposes, all Wenz curves in Fig. 4 have been raised up by 7 dB.

Figure 4 shows that across Beaufort scales 2 to 8, the PAL data and Ref. 24 are in excellent agreement and the crossover of spectral levels at high sea states has been observed in both. The PAL data in Fig. 2(a) contains Beaufort scale 9, which exhibits even more pronounced drop-off. Farmer's data[3] are in good agreement for lower sea states but slightly higher in level for Beaufort scale 5 and 8 than the other three data sets. The crossover can be observed in Figs. 4(c) and 5(d) in Farmer's data between 10 and 20 kHz.

With the 7-dB addition to the Wenz curves, they are generally consistent with the other data sets in spectral levels and shapes, but do not have the same continuously increasing wind speed ranges (limited to Beaufort 2, 3, 5, and 8) nor a uniform frequency band extending beyond 10 kHz. With data in Fig. 4(c) stopping at 3 kHz and Fig. 4(d) at 8 kHz, the Wenz data do not show the crossover as seen in Fig. 4. The data presented here are an addition to the Wenz data, with Fig. 2(a) serving as an update of the Wenz curves.

As discussed in Refs. 3 and 14 the decrease in ambient noise level with increasing wind speed can arise as bubbles are advected deeper and ambient sound is attenuated when propagating through the deeper and thicker layer of bubble plumes. A better understanding of the bubble field will help improve modeling of the bubble generation and attenuation mechanisms, which can facilitate the understanding and modeling of the sharp drop-off that occurs above 4 kHz when wind speed exceeds ∼15 m/s. Investigating the dependencies of ambient sound level on wind speed and frequency, especially the frequency dependence of the ambient noise level for wind speeds higher than 15 m/s, in relation with wind speed, wave height/direction, currents, and the bubble plume field, is part of ongoing work.

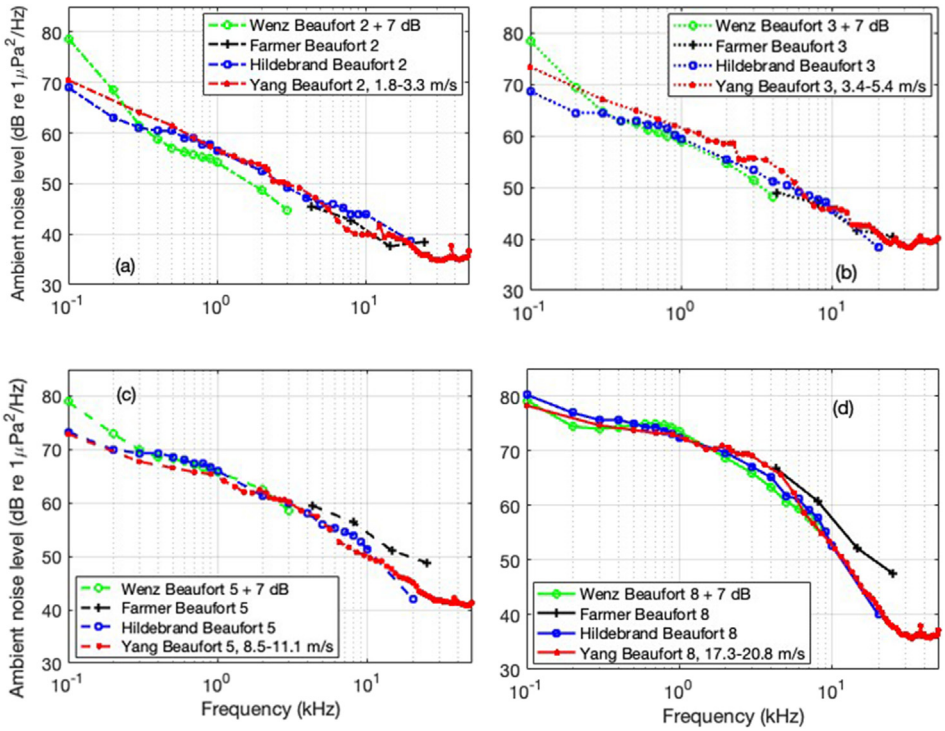

Fig. 4. Comparison between PAL and ambient noise data from Refs. 2, 3, 24, and this work under Beaufort scale 2 (a), 3 (b), 5 (c), and 8 (d). The Wenz curves are converted to units that are currently widely used with an additional 7 dB added for display purposes.

4. Summary

Two decades of ocean ambient noise data from six deep ocean moorings in the Pacific Ocean are presented. Maintained by both NOAA and NASA, these moorings provide companion wind speed and rain rate data on the surface and, therefore, provide a unique opportunity to establish the mean ambient noise level and its fluctuation due to wind forcing only.

Spanning from 1999 to 2022, data under rainy periods are first removed and the remaining data sorted under different wind speed ranges leading to sea surfaces from calm to rough. The maximum wind speed recorded is 23 m/s for the collective data set. Ambient noise levels exhibit continual increase with increasing wind speed for frequencies lower than ~4 kHz. Beyond that, the ambient noise level starts to show an increased rate of decrease as the wind speed exceeds ~15 m/s. This sharp drop-off results in a reversal in level, i.e., the ambient noise level at higher wind speed drops below that at lower wind speeds.

Representative models are discussed and two of them, Wilson's model and an approximate form of the CANARY model, that are capable of predicting absolute level, are used to compare with data presented here. Current models are similar to the Wenz curves and give predictions of a monotonic increase in ambient noise level with wind speed across all frequencies. The mismatch in data-model comparison is most likely the result of attenuation during propagation through bubble plumes as they are advected downward deeper into the water column for very rough sea states.

Comparison of ambient noise data from past work that demonstrated the spectral drop-off at high sea states, this work, and the Wenz data demonstrates consistency in spectral levels and shapes and the crossover, with the exception that the Wenz data lack sufficient coverage of both wind speed and frequency band to show the crossover. The data presented here are an addition to the Wenz data and can serve as an update of the Wenz curves.

Acknowledgments

The authors acknowledge NOAA, NASA, and ONR for their continual support over the years. This work was built on years of data collected from deep ocean moorings maintained by NOAA. The authors thank the NOAA team for their help in deploying and recovering PALs and providing high quality surface meteorological data. In particular, the authors acknowledge the Pacific Marine Environmental Laboratory of NOAA for years of field support at OCS PAPA, where the majority of the data presented here were collected. The authors acknowledge NASA for their support during the SPURS-2 field campaign. The authors also acknowledge the Office of Naval Research for supporting the data assimilation in this work. Last but not the least, the authors thank all the engineers involved in PAL related projects over the past two decades at the Applied Physics Laboratory, University of Washington for their valuable contributions to this research program.

References and links

[1]G. B. Deane and M. D. Stokes, "Scale dependence of bubble creation mechanisms in breaking waves," Nature **418**, 839–844 (2002).
[2]G. M. Wenz, "Acoustic ambient noise in the ocean: Spectra and sources," J. Acoust. Soc. Am. **34**, 1936–1956 (1962).
[3]D. M. Farmer and D. D. Lemon, "The influence of bubbles on ambient noise in the ocean at high wind speeds," J. Phys. Oceanogr. **14**, 1762–1777 (1984).
[4]D. M. Farmer and S. Vagle, "On the determination of breaking surface wave distributions using ambient sound," J. Geophys. Res. **93**, 3591–3600, https://doi.org/10.1029/JC093iC04p03591 (1988).
[5]A. Prosperetti, N. Q. Lu, and H. S. Kim, "Active and passive acoustic behavior of bubble clouds at the ocean's surface," J. Acoust. Soc. Am. **93**, 3117–3127 (1993).
[6]K. E. Trenberth and Y. Zhang, "How often does it rain?," Bull. Am. Meteorol. Soc. **99**, 289–298 (2018).
[7]B. Ma and J. A. Nystuen, "Passive acoustic detection and measurement of rainfall at sea," J. Atmos. Oceanic Technol. **22**, 1225–1248 (2005).
[8]J. Yang, S. C. Riser, J. Nystuen, W. E. Asher, and A. T. Jessup, "Regional rainfall measurements using Passive Aquatic Listener during SPURS field campaign," Oceanography **28**, 124–133 (2015).
[9]S. C. Riser, J. Yang, and R. Drucker, "Observations of large-scale rainfall, wind, and sea surface salinity variability in the eastern tropical Pacific," Oceanography **32**, 42–49 (2019).
[10]J. A. Nystuen, "Rainfall measurements using underwater ambient noise," J. Acoust. Soc. Am. **79**, 972–982 (1986).
[11]B. Ma, J. A. Nystuen, and R. C. Lien, "Prediction of underwater sound levels from rain and wind," J. Acoust. Soc. Am. **117**, 3555–3565 (2005).
[12]NOAA Tropical Atmosphere Ocean (TAO) data link, https://www.pmel.noaa.gov/gtmba/pmel-theme/pacific-ocean-tao (Last viewed February 21, 2023).
[13]NOAA Ocean Climate Stations (OCS) data link, https://www.pmel.noaa.gov/ocs/data-overview (Last viewed February 21, 2023).
[14]S. Vagle, W. G. Large, and D. M. Farmer, "An evaluation of the WOTAN technique for inferring oceanic wind from underwater sound," J. Atmos. Oceanic Technol. **7**, 576–595 (1990).
[15]B. F. Cron and C. H. Sherman, "Spatial correlation functions for various noise models," J. Acoust. Soc. Am. **34**, 1732–1736 (1962).
[16]D. Chapman, "Surface-generated noise-in shallow water: A model," in *Proceedings of the Institute of Acoustics* (1987), Vol. 9, pp. 1–11.
[17]M. J. Buckingham, "A theoretical model of ambient noise in a low-loss shallow water channel," J. Acoust. Soc. Am. **67**, 1186–1192 (1980).
[18]A. Plaisant, "Spatial coherence of surface generated noise," in *Proceedings of Underwater Defense Technology*, Microware Exhibitions and Ltd., Kent, UK (1992), pp. 515–522.
[19]W. A. Kuperman and F. Ingenito, "Spatial correlation of surface generated noise in a stratified ocean," J. Acoust. Soc. Am. **67**, 1988–1996 (1980).
[20]J. E. Breeding, Jr., L. A. Pflug, M. Bradley, M. H. Walrod, and W. McBride, "Research ambient noise directionality (RANDI) 3.1 physics description," Naval Research Laboratory Report No. NRL/FR/7176-95-9628 (1996).
[21]C. H. Harrison, "CANARY: A simple model of ambient noise and coherence," Appl. Acoust. **51**, 289–315 (1997).
[22]J. H. Wilson, "Wind-generated noise modelling," J. Acoust. Soc. Am. **73**, 211–216 (1983).
[23]H. Medwin and M. M. Beaky, "Bubble sources of the Knudsen sea noise spectra," J. Acoust. Soc. Am. **86**, 1124–1130 (1989).
[24]J. A. Hildebrand, K. E. Frasier, S. Baumann-Pickering, and S. M. Wiggins, "An empirical model for wind-generated ocean noise," J. Acoust. Soc. Am. **149**, 4516–4533 (2021).
[25]R. J. Urick, *Principles of Underwater Sound*, 3rd ed. (Peninsula, Westport, CT, 2010), pp. 14–15.